For submission to Water Supply as a Research Paper

Development of the simple analytical method for determination of Arsenate(V) ion using fluorescence-labeled DNA and Cerium oxide nanoparticles

Koji Matsunaga[a,*], Hisashi Satoh[a], Reiko Hirano[b],

[a] Division of Environmental Engineering, Faculty of Engineering, Hokkaido University, North-13, West-8, Sapporo 060-8628, Japan

[b] Cellspect Co., Ltd., 1-10-82 Kitaiioka, Morioka, Iwate, 020-0857, Japan

E-mail addresses:

Koji Matsunaga: k-matsunaga_7dnd@eis.hokudai.ac.jp

Hisashi Satoh: qsatoh@eng.hokudai.ac.jp

Reiko Hirano: hirano0317@gmail.com

[*] *Corresponding author*: Koji Matsunaga

Tel. & Fax: +81-11-706-6277

19 E-mail: k-matsunaga_7dnd@eis.hokudai.ac.jp

20

Abstract

Arsenic (As) contamination in groundwater presents a major health and environmental concern. As is found in two oxidation states and most chemical tests for inorganic arsenic are focused on As(III), and few have been developed for As(V). We developed the simple analytical method for determining As(V) concentrations in groundwater using CeO_2NPs and fluorescein (FAM)-labeled DNA. Prior to sample measurements, we investigated the key operational parameters that affect the sensing performance. The optimal CeO_2NPs final concentration, FAM-labeled DNA final concentration, the sequence and length of FAM-labeled DNA, and incubation time were 15 μg/mL, 400 nM, 6-mer poly-cytosine sequence, and 6 min, respectively. After optimizing the parameters, the total analysis time was about 20 min and the limit of detection was 0.61 μM. This method has a high selectivity against the same concentrations of Cu(II), Cd(II), Hg(II) and Pb(II). Pretreatment by cation extraction to remove interfering ions was beneficial for determination of As(V) concentrations in groundwater containing a variety of metal cations at high concentration. We could determine As(V) concentration in groundwater. Modification of the reactions of the method is necessary. This study provides the first step in the development of a simple

method for on-site As(V) analysis.

Keywords: Arsenate; Groundwater; Nanoparticles; Single-stranded DNA; Simple analytical method

Highlights

- Cerium oxide nanoparticles-based fluorescence method for As(V) determination was developed.
- Parameters that influence the method were optimized.
- Most of groundwaters could determine As(V) concentrations roughly.

Introduction

Inorganic arsenic (As) is extremely toxic, leading to a serious threat including cardiovascular, respiratory diseases, and cancers of skin, lung, liver and kidney (Chung, Huang, et al., 2013; Singh, Singh, et al., 2015; Flora, 2015). Its contamination of drinking water sources was estimated to affect human health over 144 million people around the world (Clancy, Hayes, et al., 2013). Because of high toxicity of As, the World Health Organization (WHO) and the US Environmental Protection Agency (USEPA) set the primary maximum contaminant level (MCL) for total As in drinking water as low as 10 μg/L (WHO, 2011; USEPA, 2018). Chowdhury *et al.* reported that more than 100 μg/L-As concentrations have been detected in about 47.9% of well water and the lower As concentrations is less than 10 μg/L and the upper As concentrations is higher than 1000 μg/L in Bangladesh (Chowdhury, Biswas, et al., 2000). Amini *et al*. modeled probability maps of global As contamination using a large database of measured As concentration in groundwaters from around the world and the digital maps of physical characteristics such as soil, geology, climate and elevation (Amini, Abbaspour, et al., 2008). They showed that most of countries could contaminate As higher than 10 μg/L (Amini, Abbaspour, et al., 2008).

Some commercial instruments which are commonly used for As determination include atomic absorption spectrometry (AAS), atomic fluorescence spectrometry and inductively coupled plasma mass spectrometry (ICP-MS), hydride generation atomic absorption spectrometry (HG-AAS), electrothermal atomic absorption spectrometry (ETAAS), flow injection-hydride generation-inductively coupled plasma mass spectrometry (FI-HG-ICPMS), anodic stripping voltammetry (ASV), cathodic stripping voltammetry (CSV) using a hanging drop mercury electrode (Das and Sarkar, 2016). Although these traditional techniques have excellent accuracy and sensitivity, they require sophisticated, expensive and bulky equipment, specialized expertise for operation, and high operating cost. Hence, they are not suitable to on-site analysis (Wu, Liu, et al., 2012a; Kaur, Kumar, et al., 2015).

Inorganic As has two common oxidation states: arsenate (As(V)) and arsenite (As(III)). Most of chemical and biological sensors have been developed to determine As(III) (Baghbaderani and Noorbakhsh, 2019) or total As based on using DNA aptamer (Matsunaga, Okuyama, et al., 2019; Zhan, Yu, et al., 2014; Wu, Liu, et al., 2012b) or the redox properties and strong thiophilicity of As (Pena-Pereira, Villar-Blanco, et al., 2018; Xu, Wang, et al., 2019). However, those assays could not determine As(V) alone although some commercial kits are available for As detection. They rely on the reduction of As(III)

86 species in solution by zinc to form arsine gas (Lopez, Zhang, et al., 2017). While it is
87 more challenging to detect As(V) alone, there are a few studies to detect As(V) have also
88 been developed, which use polymer hydrogels, small molecules, gold nanoparticles, and
89 bimetallic NPs (Lopez, Zhang, et al., 2017).

90 Recently, there has been interests in using nanomaterials for analytical
91 applications. The nanomaterials in general have a high specific surface area and may offer
92 high sensitivity. One of the nanomaterials is metal oxide nanoparticles (MONPs). The
93 MONPs were carried out for their ability to adsorb DNA, quench fluorescence (Pautler,
94 Kelly, et al., 2013), and release DNA in the presence of target anions (Liu and Liu, 2015).
95 DNA-functionalized MONPs might be useful as a sensor platform for anion detection. In
96 previous studies, iron oxide nanoparticles (Fe_3O_4NPs) are used as the As(V) sensor
97 because As(V) binds to Fe_3O_4NPs surface (Liu and Liu, 2014; Liu and Liu, 2015).
98 Another studies showed that cerium oxide nanoparticles (CeO_2NPs) were a general
99 oxidase that could oxidize many substrates (Pautler, Kelly, et al., 2013). CeO_2NP also
100 adsorbed As(V) on its surface and its DNA adsorption affinity was stronger than that of
101 Fe_3O_4NP (Liu and Liu, 2015; Lopez, Zhang, et al., 2017; Bülbül, Hayat, et al., 2018).
102 However, their application for environmental monitoring has been extremely limited
103 because of the lack of selectivity (Lopez, Zhang, et al., 2017; Muppidathi, Perumal, et al.,

2019). Here, we developed a simple analytical method for determination of As(V) concentrations in various kinds of groundwater by fluorescence spectroscopy.

Materials and methods

Principle

Scheme 1 shows the sensing mechanism of the method. First, fluorescein (FAM)-labeled DNA is incubated with CeO_2NPs. FAM-labeled DNA is adsorbed onto the CeO_2NP surface and the fluorescence might be quenched. Second, samples are added into the solution. In the absence of As(V), FAM-labeled DNA-CeO_2NPs complex remains in the solution. In contrast, As(V) displaces the adsorbed FAM-labeled DNA from the CeO_2NPs, resulting in recovery of fluorescence signal. Therefore, a quantitative analysis of the As(V) concentration is possible by measuring the fluorescence intensity derived from FAM (Ex: 495 nm, Em: 520 nm).

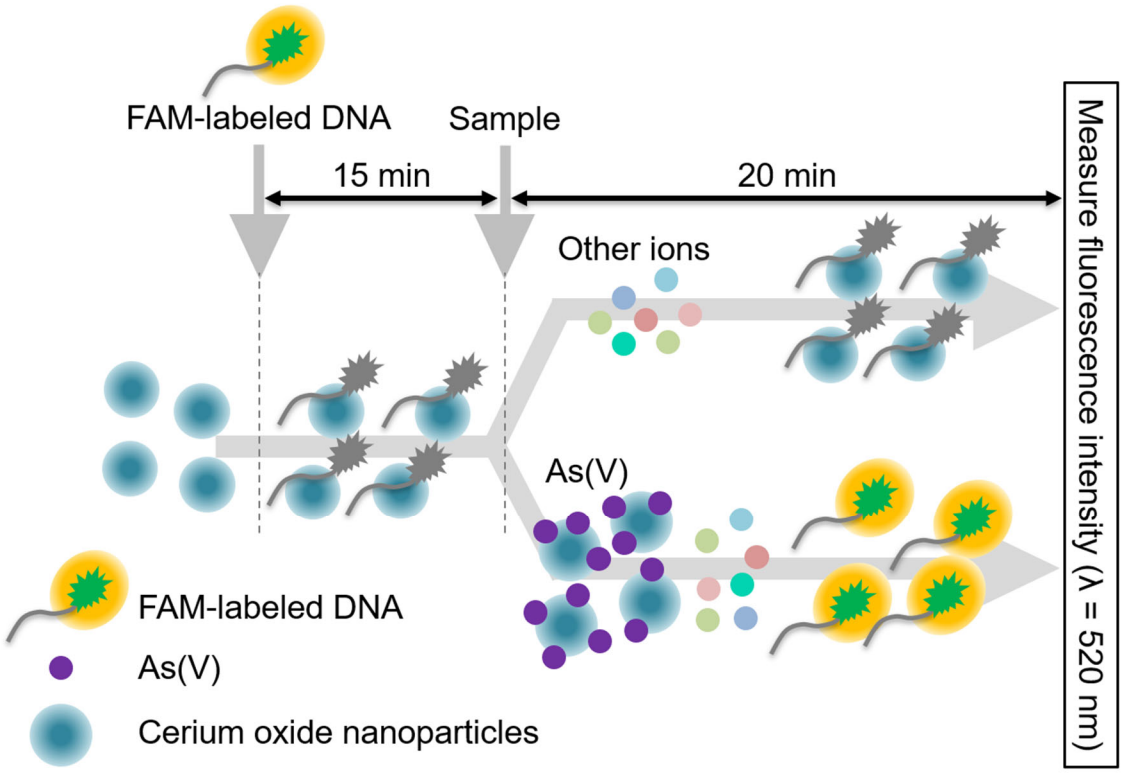

Scheme 1: Schematic representation of the colorimetric detection of As(V) in aqueous solution based on an FAM-labeled ssDNA and cerium oxide nanoparticles.

Chemicals and materials

All of the FAM-labeled DNA were from Eurofins Genomics K.K. (Tokyo, Japan). Table 1 shows the list of sequence which were used in this study. 4-(2-hydroxyethyl)-1-piperazineethanesulfonic acid (HEPES) was from Nakalai tesque, INC. (Kyoto, Japan). CeO_2NPs as a 10 wt.% in H_2O (catalogue number 643009-100ML) was from Sigma-Aldrich Japan (Tokyo, Japan). As(V) as a 60% arsenic acid solution (H_3AsO_4, catalog

number 013-04675) was from Fujifilm Wako Pure Chemical Corporation (Osaka, Japan). All solutions were prepared with Milli-Q Water (Merck Millipore, Tokyo, Japan).

Table 1. The DNA sequences which we used in this study.

DNA Name	Sequences
FAM-C_6	5′-[FAM]-CCCCCC-3′
FAM-C_{12}	5′-[FAM]-CCCCCCCCCCCC-3′
FAM-C_{18}	5′-[FAM]-CCCCCCCCCCCCCCCCCC-3′
FAM-C_{24}	5′-[FAM]-CCCCCCCCCCCCCCCCCCCCCCCC-3′
FAM-C_{30}	5′-[FAM]-CCCCCCCCCCCCCCCCCCCCCCCCCCCCCC-3′

Determination of As(V) using CeO_2NPs and FAM-labeled ssDNA

The probe solution was prepared by adding CeO_2NPs dispersion and FAM-labeled DNA solution to the 10-mM HEPES buffer solution (pH: 7.6). After 15 minutes, a 20-μL probe solution was added into the microtubes. A 20-μL sample solution was mixed with the probe solution in the microtube. After incubation of the mixture at room temperature for 20 min, the fluorescence intensity at 518 nm in the test solution was

142 measured.

143 We examined the effects of the concentrations of CeO_2NPs and FAM-labeled
144 ssDNA, the length of FAM-labeled ssDNA and the incubation time with samples on the
145 method sensitivity. To optimize the concentration of CeO_2NPs and FAM-labeled ssDNA,
146 the final CeO_2NPs concentrations of the test solutions were changed from 0 to 60 μg/mL
147 and the final FAM-labeled ssDNA concentrations were changed from 0 to 500 nM after
148 the optimization of final CeO_2NPs concentration. We compared the fluorescence intensity
149 at 518 nm of the sample with 1-μM As(V) (POS) and one without As(V) (NEG). To
150 optimize the length of the DNA, FAM-labeled poly-cytosine DNAs (Table 1) were used
151 to study As(V)-induced DNA detachment reaction. All of the data were used to calculate
152 ΔF, which is the difference between the fluorescence intensity of the POS and the NEG
153 samples. To optimize the incubation time after adding the samples, three test solutions of
154 the POS and the NEG samples, respectively, were incubated for 30 min after adding the
155 sample, and the fluorescence intensities were measured every 6 min and ΔF were
156 calculated.

157 After optimization of the parameters described above, we created a calibration
158 curve of the method at a variety of As(V) concentrations. The fluorescence spectra of ten
159 blank samples (using Milli-Q water as the samples) and three samples of As(V) standard

160 solution at individual As(V) concentrations were measured. The fluorescence peaks at
161 518 nm were plotted against the corresponding As(V) concentrations. A linear regression
162 was also used to obtain a calibration curve at As(V) concentrations above 0.5 μM. Based
163 on the results, the limit of detection (LOD) value was estimated using an equation, 3σ/s,
164 where σ is the standard deviation of ten blank samples and s is a slope of the regression
165 line.

166 Selectivity of the method was assessed by measuring the fluorescence intensities
167 of the test solutions with H_3AsO_4, $NaAsO_2$, H_3BO_3, $NaHCO_3$, Na_2CO_3, $NaNO_3$, NaF,
168 K_2HPO_4, Na_2SO_3, Na_2SO_4, Na_2SeO_4, KBr and KI at 10 μM, which were against As(V)
169 for the environmentally important anions. For the cations, we used NaCl, $MgCl_2 \cdot 6H_2O$,
170 KCl, $CaCl_2$, $MnCl_2 \cdot 4H_2O$, $FeCl_2 \cdot 4H_2O$, $FeCl_3 \cdot 6H_2O$, $CoCl_2$, $NiCl_2 \cdot 6H_2O$, $CuCl_2 \cdot 2H_2O$,
171 $ZnCl_2$, $HgCl_2$ and $(CHCOO)_2Pb \cdot 3H_2O$ as the selectivity test. ΔF were compared among
172 these samples by Steel test.

173 Groundwater samples (GW) were taken in February 2019. Since the GW did not
174 contain As, As(V) was spiked to the GW at different concentrations for determination
175 tests. The samples were filtered through a 0.2-μm pore-size membrane (Advantec Co.,
176 Ltd., Japan) and then passed through a cation-exchange column (MetaSEP IC-MC, GL
177 Sciences, Tokyo, Japan). Thereafter, As(V) concentrations were determined by using our

178 method and ICP-MS and HPLC-ICP-MS and both were compared.

179

180 *Instrumentation and software*

181

182 The fluorescence intensity was measured by using a fluorescence
183 spectrophotometer FP-6600 (JASCO Corporation, Tokyo, Japan). The metal-ion
184 concentrations in groundwater were measured by ICP-MS 8800 ICP-QQQ (Agilent,
185 United States) and HPLC-ICP-MS system, which were passed through a GelPack GL-
186 IC-A column (Hitachi Chemical) connected to a high performance liquid chromatograph
187 (Shimadzu, SLC-10Avp system), and introduced to an inductively coupled plasma mass
188 spectrometer (ICP-MS, Thermo, iCAP Qc) (Kamei-Ishikawa, Segawa, et al., 2017). R
189 version 3.5.2 was used for the statistical analysis in this study.

190

191 **Results and Discussion**

192

193 *Effect of CeO_2NPs and FAM-labeled DNA concentrations on fluorescence intensity*

194

Because the CeO_2NPs and FAM-labeled ssDNA concentrations are the most important of all parameters, the effect of final CeO_2NPs concentration and FAM-labeled DNA concentration on the fluorescence intensity were investigated. Figure 1 shows the effect of the final CeO_2NPs concentrations on fluorescence intensity of the POS and NEG samples. The fluorescence intensity decreased as the concentration of CeO_2NPs increased in both samples. Only at 15 μg/mL of CeO_2NP concentrations, the fluorescence intensity of the POS sample became higher than the NEG sample and there was statistically significant difference ($p = 0.05$). Because the difference in fluorescence intensity of the POS and NEG samples is related to the sensitivity of the method, the final CeO_2NPs concentration of a test solution was determined to be 15 μg/mL.

205

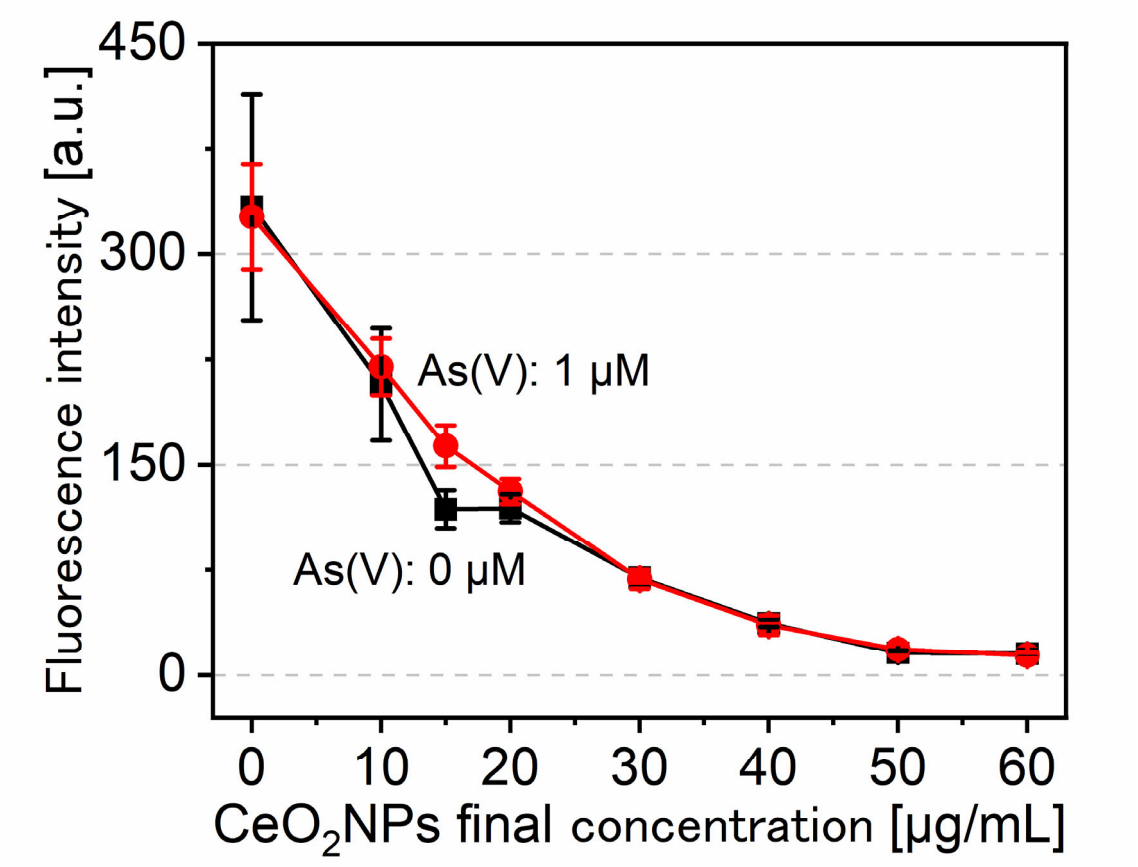

206

207 Figure 1: Effect of the final CeO_2NPs concentrations of the test solutions on

208 fluorescence intensity in the presence (POS) and absence of As(V) (NEG). FAM-C_6 as

209 FAM-labeled ssDNA was used. The final FAM-C_6 concentration was 375 nM. The

210 incubation time after sample addition was 20 min.

211

212 At 0-10 µg/mL, there were no difference between POS and NEG due to the low

213 amount of As(V) detached. At 20 µg/mL or higher, the amount of CeO_2NPs was higher

than that of FAM-C_6 in the test solution. We thought it is because the pentavalent As adsorbed on the free CeO_2NPs and was not desorbed by adding FAM-C_6.

We performed the adsorption equilibrium experiments to calculate the detachment constant (K_d) of the FAM-labeled ssDNA from CeO_2NPs. In the adsorption equilibrium experiments, a 20-μL aliquots of the probe solution were added into 1.5-mL tubes. The probe solution was prepared by adding CeO_2NPs dispersion (0-60 μg/mL) and FAM-labeled ssDNA solution (400 nM) to the 10-mM HEPES buffer solution (pH: 7.6). 10-mM HEPES buffer solution (pH: 7.6) was prepared as a control sample. After measuring the fluorescence intensity, we calculated the concentration of adsorbed ssDNA using the calibration curve of the fluorescence intensity at 518 nm versus the concentration of FAM-labeled DNA. The obtained data were fitted to the Langmuir models using Equation (1) (Hafuka, Nagasato, et al., 2019);

$$q_e = Q_m b C_e / (1 + b C_e) \quad (1)$$

where q_e is the concentration of ssDNA that adsorbed onto CeO_2NPs (nM), C_e is the equilibrium concentration of non-adsorbed ssDNA (nM), Q_m is the maximum adsorption capacity of ssDNA (nM) and b is the constant related to the energy of adsorption. As a result, the binding curve was fitted to the plots of the NEG samples and the K_d of DNA from CeO_2NPs was calculated to be 5.17 μg/mL (Figure S1).

We also optimized the final FAM-labeled ssDNA concentration (Figure 2). The difference of fluorescence intensity of the POS and NEG samples increased as the final concentration of FAM-labeled DNA was increased. The ΔF were the highest (75.2) at 400 nM of FAM-labeled ssDNA. It decreased when FAM-labeled ssDNA concentration was 500 nM, but we considered that it was a measurement error because there was no statistically significant difference ($p = 0.05$) between the results at 400 nM and 500 nM. Based on these results, the final concentration of FAM-labeled DNA was determined to be 400 nM.

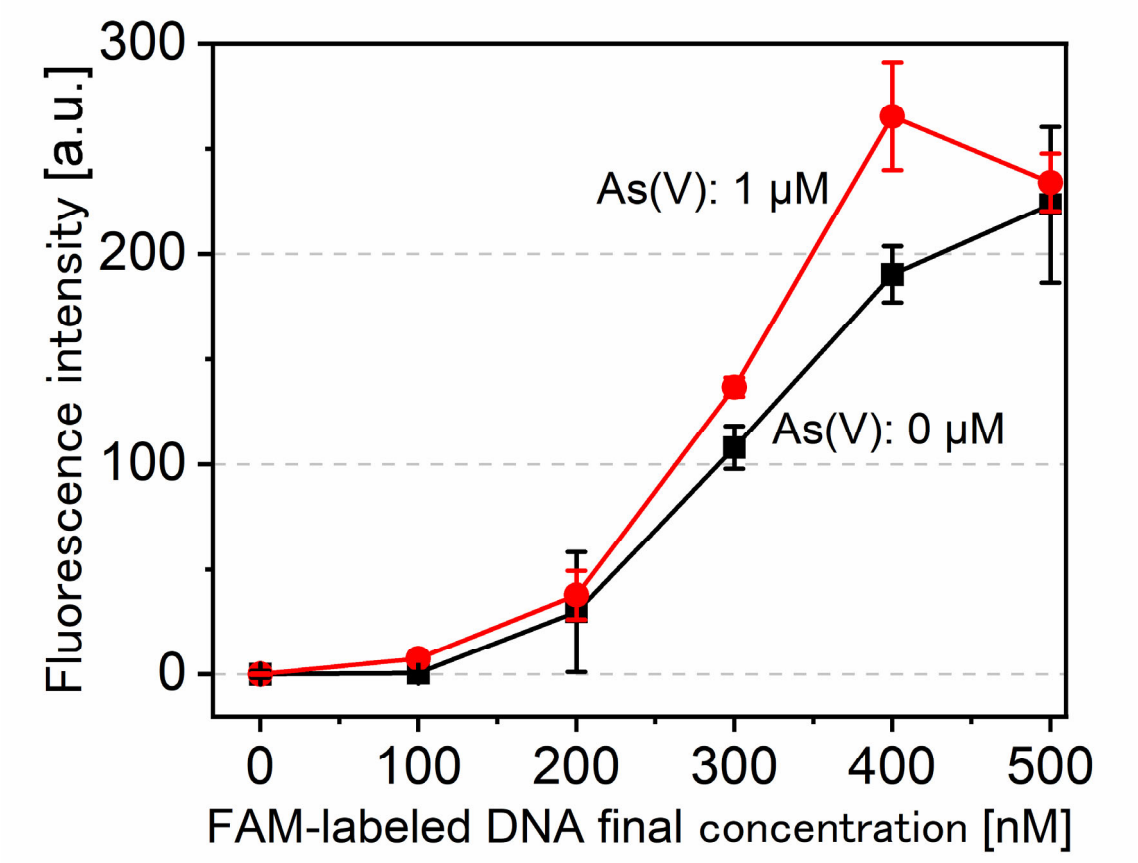

Figure 2: Effect of final FAM-labeled DNA concentration of test solutions on fluorescence intensity in the POS and NEG. The final CeO_2NPs concentration was 15 μg/mL, FAM-C_6 as FAM-labeled DNA was used and the incubation time after sample addition was 20 min.

Effect of the length of FAM-labeled DNA on fluorescence intensity

It was expected that the ssDNA length would affect the As(V)-induced ssDNA detachment reaction (Liu and Liu, 2014). Therefore, we investigated the effect of ssDNA length on ΔF. We used FAM-C_n (n changes from 6 to 30) (Figure 3). The previous studies have shown that adsorption took place via the phosphate backbone (Lopez, Zhang, et al., 2017; Liu and Liu, 2014). Moreover, C_6 had the highest adsorption and detachment affinity among four types of bases (Lopez, Zhang, et al., 2017; Liu and Liu, 2014). We found that the fluorescence intensity increased as the As(V) concentration increased (Figure 3) due to the FAM-C_6 adsorbed onto CeO_2NPs was detached (Scheme 1). The ΔF of the POS samples with C_{12} to C_{30} did not increase as the As(V) concentration increased due to C_{12} and longer ones adsorbed too tightly onto CeO_2NPs surfaces to detach. The FAM-C_6 could produce a higher sensitivity because it was easier to the adsorbed than the FAM-C_{12} and the longer ones. Previous studies showed that FAM-A_{15} was used for MnO_2NPs (Wang, Huang, et al., 2018) and FAM-C_{15} were used for Fe_3O_4NPs (Liu and Liu, 2014) to achieve fluorescence quenching and recovering. We concluded that CeO_2NPs have the unique property to achieve higher sensitivity using shorter FAM-labeled DNA length.

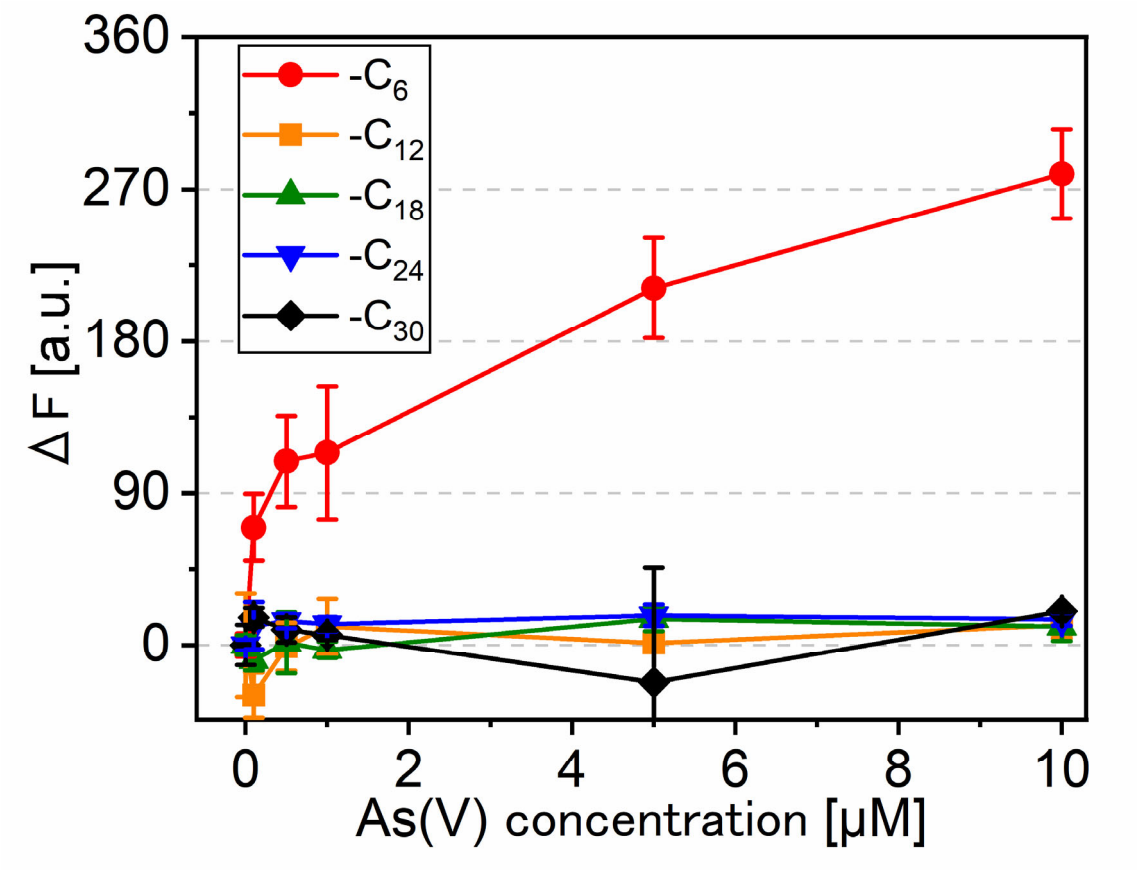

Figure 3: Effect of DNA length on calibration curves. The final CeO_2NPs concentration was 15 μg/mL, the final concentration of each FAM-labeled DNA was 400 nM and the incubation time after sample addition was 20 min.

Effect of the incubation time after adding samples on fluorescence intensity

Figure 4 shows the time course change in ΔF. The ΔF increased immediately within the initial 6 min, indicating that the detachment of FAM-labeled ssDNA from

275 CeO_2NPs occurred within the initial 6 min. The ΔF maximum value at 18 min. In

276 contrast, the ΔF did not increase until 18 min and increased thereafter. Based on these

277 results, the optimal incubation time after sample addition was determined to be 6 min.

278 The optimal incubation time was shorter than that in the previous studies using

279 Fe_3O_4NPs and MnO_2NPs (over 30 min) (Liu and Liu, 2014; Wang, Huang, et al., 2018).

280 Such fast signaling kinetics is advantageous for analysis of As(V). This is likely because

281 the density of FAM-C_6 on the CeO_2NPs surface was higher than Fe_3O_4NPs and

282 MnO_2NPs, which would accelerate the displacement reaction.

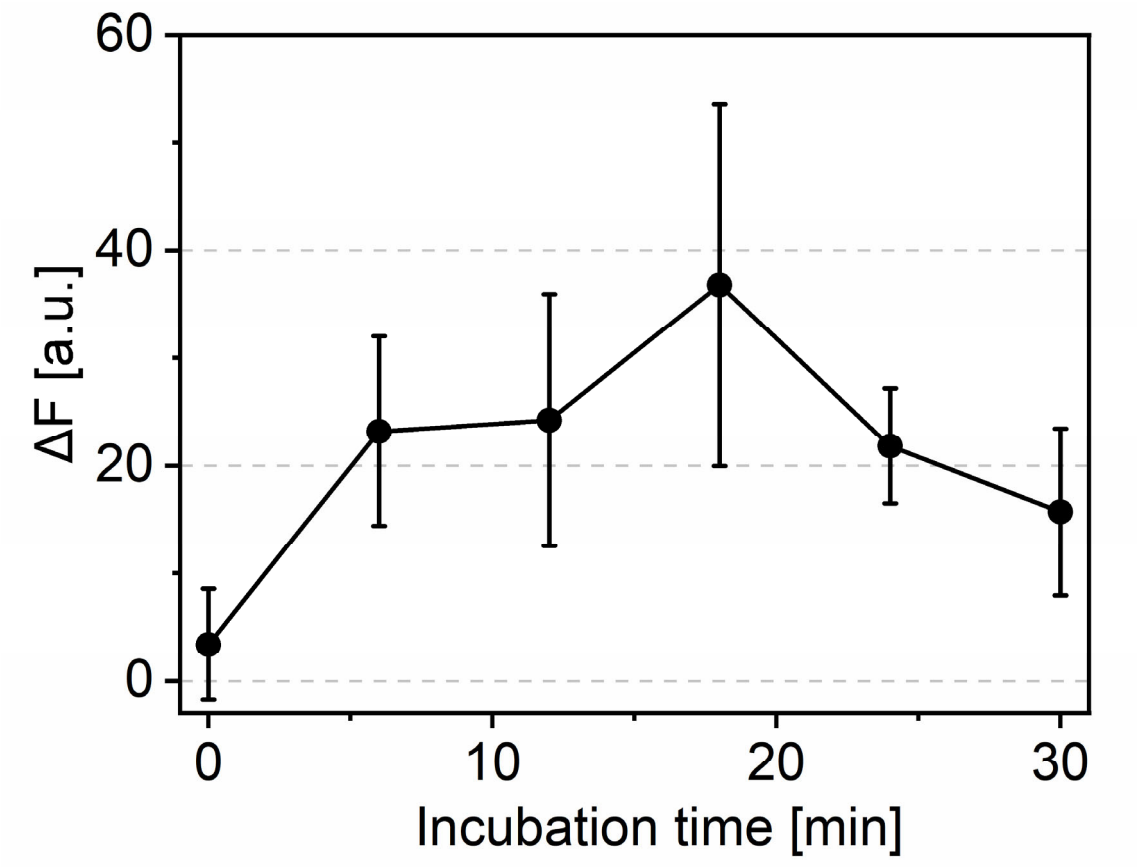

283

Figure 4: Variation of ΔF of test solutions with time after sample addition in the POS and NEG. The final CeO_2NPs concentration was 15 µg/mL, FAM-C_6 as FAM-labeled DNA was used and the final FAM-C_6 concentration was 400 nM.

Calibration Curve

Figure 5 shows a calibration curve of As(V) for the method. The ΔF of the test solutions remained unchanged below 0.5 µM As(V) and logarithmically increased from 40 to 200 with increase in As(V) concentrations from 0.5 to 2 µM. The detection limit (LOD) was calculated to be 0.61 µM. When the As(V) concentration exceeded 2 µM, the ΔF increased further and remained almost unchanged at 50 µM As(III) (data not shown).

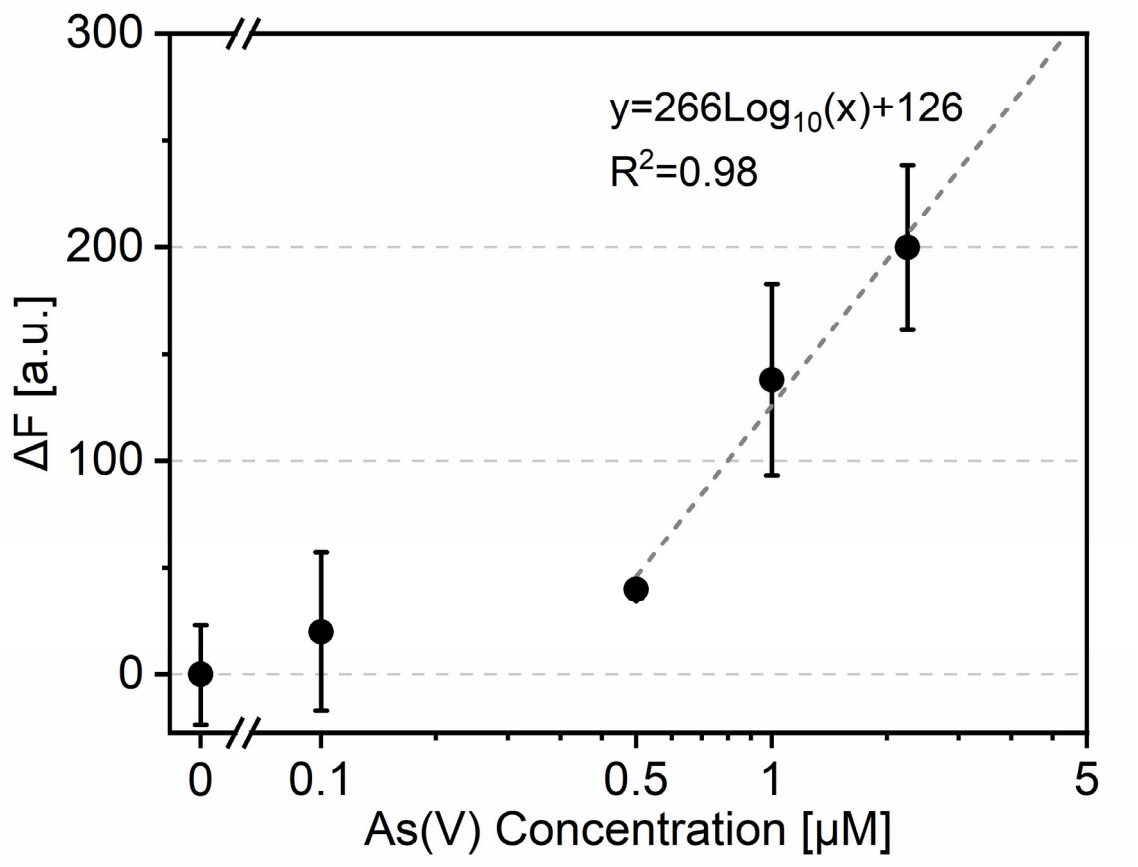

Figure 5: Method calibration curve. The dotted line is a regression line.

Method Selectivity

Figure 6 shows the ΔF of the samples with different anions. The ΔF of the solution with As(V) was significantly higher than that of the blank sample. The ΔF of the samples with sulfate were slightly higher and the samples with carbonate and phosphate were slightly lower than that of the blank sample. We conducted a statistical analysis among the anions. There were no statistically significant differences ($p > 0.05$)

among blank and the other anions (except As(V)). However, when the inhibitory test was conducted using 100 μM of the anions, borate and phosphate interfered the method (Figure S2). When we made the calibration curve of the method using borate and phosphate instead of As(V), the fluorescence intensity increased with increase in these anions (Figure S3). Therefore, we found that borate and phosphate were the main interfering substances in this method.

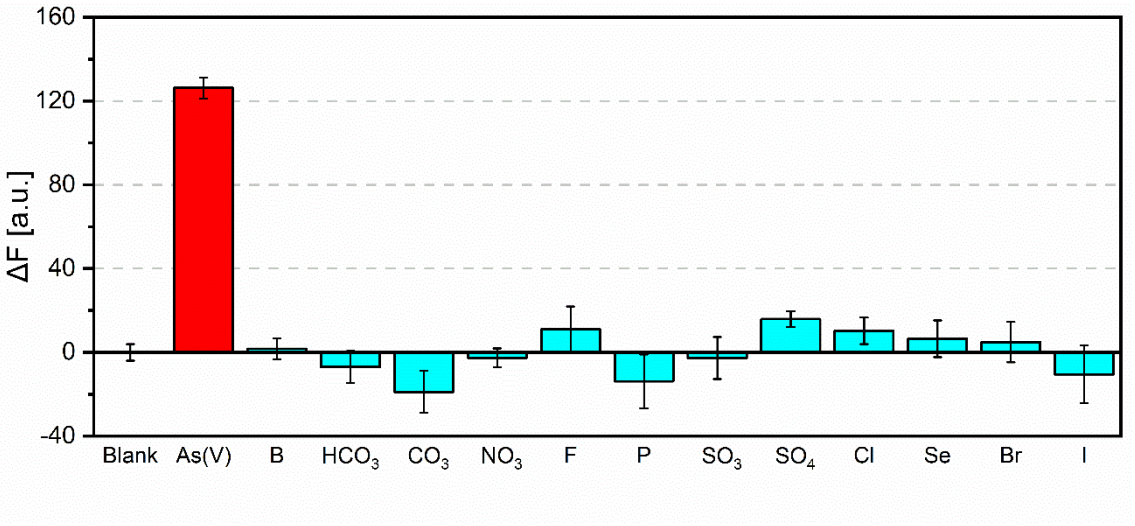

Figure 6: Method selectivity for anions. The concentration of anion was 10 μM.

Figure 7 shows the ΔF of the samples with different cations. The ΔF of the solution with As(V) was significantly higher than that of the blank sample. There were no statistically significant differences ($p = 0.05$) in the ΔF of the samples with As(III), K(I), Ca(II), Mn(II), Fe(II), Fe(III), Co(II) and Ni(II) solutions against the blank sample. In contrast, ΔF values were slightly higher in the solutions of Na(I), Mg(II), Fe(III) and

Zn(II) and significantly higher in the solutions with Cu(II), Cd(II), Hg(II) and Pb(II). However, we could remove these ions by pre-treatment applied in this study (see Figure S4). These results showed a high selectivity of the method toward As(V) after the pre-treatment.

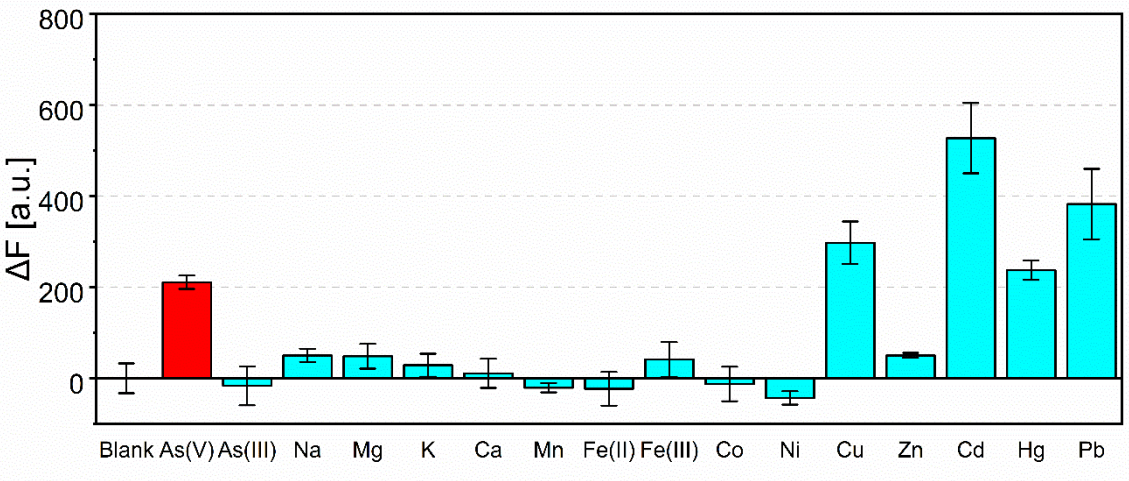

Figure 7: Method selectivity for cations including As(V) and As(III). The concentration of each ions was 10 µM.

Analysis of Groundwater Samples

Contrary to expectations, when GW without As(V) was subjected to the assay, the peak of fluorescence intensity at 518 nm increased significantly (Figure 8). The increase in the fluorescence band might be attributed to detachment of the FAM-C_6 by the ions in the sample (Table S1). Therefore, the GW was pretreated with a 0.2-µm-

pore-size membrane filter and cation-exchange resin. Membrane filtration did not remove the interfering ions in the GW (Figure 8). In contrast, the peak of fluorescence intensity of the sample subjected to filtration followed by cation exchange almost same as that of a blank sample (Figure 8), indicating that the filtration followed by cation exchange could significantly reduce interfering effects of matrix of GW. Table S1 shows the ion concentrations in the GW before and after cation-exchange treatment. The GW contained divalent cations (*i.e.*, Mg(II) and Ca(II)), which might explain increasing the peak of fluorescence band (Figure S5). The results show that metal-cation concentrations in GW were efficiently removed by cation exchange and alternatively Na(I) was released.

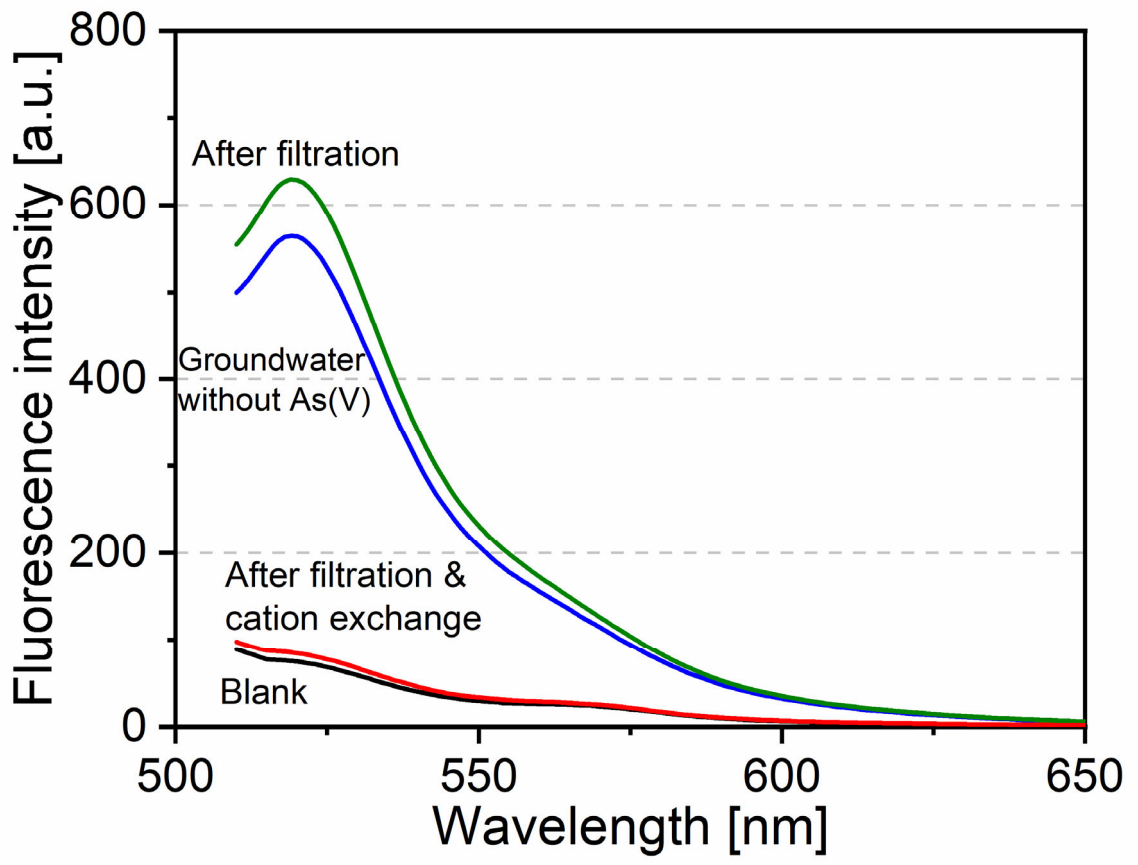

Figure 8: Fluorescence intensity of FAM-labeled DNA in groundwater, groundwater filtered with 0.2-μm-pore-size membrane filter, and groundwater filtered with 0.2-μm-pore-size membrane filter and passed through cation-exchange resin.

Figure 9 shows the relationship between the concentrations of As(V) in GW determined by the method and HPLC-ICP-MS. Some plots show that As(V) concentrations determined by the method were almost identical to those by HPLC-ICP-MS. Our methods could determine As(V) concentration in groundwater between 0.1 μM and 1.0 μM. On the other hand, our methods could not determine As(V) concentration

in groundwater above 2.5 μM because the standard deviations were larger and greatly overestimated (data not shown).

However, As(V) concentrations of most of the samples have the large measurement error because Na(I) was sole ions present in the pre-treatment samples (Table S1) and standard error of the results was large. Therefore, we need to modify the method to reduce the measurement error.

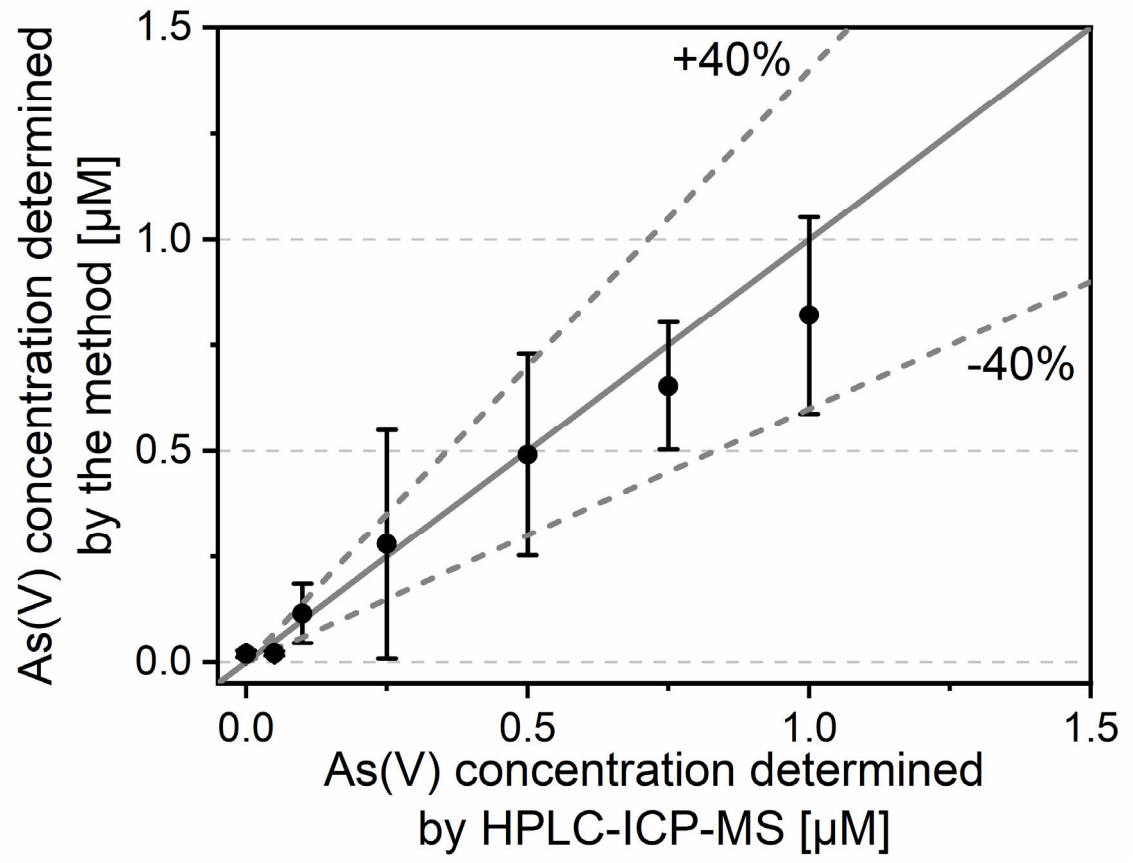

Figure 9: Relationship between concentrations of As(V) determined by HPLC-ICP-MS and those determined by using the method.

Lakatos *et al*. developed the simple analytical method for As(V) using S-layer functionalized gold nanoparticles (Lakatos, Matys, et al., 2015). Das *et al*. developed the As(V) sensor based on antimonyl–arseno–molybdate complex in the presence of ammonium molybdate, potassium antimonyl tartrate and ascorbic acid (Das and Sarkar, 2016). However, As(III) is also adsorbed onto gold nanoparticles (Zong and Liu, 2019) and the selectivity between As(III) and As(V) is not shown in the study (Lakatos, Matys, et al., 2015). The As(V) sensor which Das et al. developed can measure As(V) concentration by color shading, which is not suitable for low concentration As(V) analysis because the LOD is higher than that of our method (Das and Sarkar, 2016).

The merit of our method is that it is selective for As(III). It is because the simple analytical methods for As have been developed only for As(III) and total As, but not for As(V). On the other hand, the disadvantage of our method is that it is subject to interference by other anions such as borate and phosphate at high concentrations. Since there is no simple technique to separate As(V) from borate and phosphate, our method cannot be applied to samples with high concentrations of borate and phosphate.

Determining various chemical species such as As(III) and As(V) is a quite challenging task. The instrumental methods, such as LC-ICP-MS, are not common to determine the concentration of various As species. In this regard, developing the

methods for analysis of various As species is of importance. Our method relies on the strong interaction between As(V) and the surface of metal oxide nanoparticles and provides an inexpensive, simple, and easy-to-use platform.

Conclusion

In this study, we developed a simple analytical method to determine As(V) concentrations using CeO_2NPs and a FAM-labeled ssDNA and firstly attempted to measure the concentration of As(V) in groundwater by the method. The parameters that affect the method performance, such as the final concentration of CeO_2NPs (15 μg/mL) and FAM-labeled DNA (400 nM), the sequence and length of FAM-labeled DNA (FAM-C_6) and incubation time (6 min-) with samples were optimized. After optimizing the parameters, the total analysis time was about 20 min and the LOD was 0.61 μM. This method has a significant selectivity against the same concentrations of Cu(II), Cd(II), Hg(II) and Pb(II) and a slight selectivity against the same concentrations of sulfate and carbonate. For cations, pre-treatment by cation extraction to remove interfering ions was beneficial for determination of As(V) concentrations in groundwater containing a variety

of metal cations at high concentration. We could underestimate the As(V) concentrations in As(V)-spiked GW by the method. In the future, we should reduce the standard deviation and stabilize the adsorption and detachment of FAM-labeled DNA and As(V) onto CeO_2NPs. This method has the potential in the development of an As(V) sensor for application to on-site analysis.

Acknowledgements

This research was supported financially by JSPS KAKENHI [grant number 21H04568, 20KK0090, 17H03328, 26289178, 23686074], and the Matching Planner Program from Japan Science and Technology Agency [grant number JPMJTM15KU]. We thank Prof. Ayumi ITO and Ms. Yumi Kawamura for As measurements by HPLC-ICP-MS.

References

Amini, M., Abbaspour, K. C., Berg, M., Winkel, L., Hug, S. J., Hoehn, E., Yang, H., and Johnson, C. A. (2008) Statistical Modeling of Global Geogenic Arsenic Contamination in Groundwater. Environmental Science & Technology, **42**(10), 3669–3675. [online] http://dx.doi.org/10.1021/es702859e.

Baghbaderani, S. S. and Noorbakhsh, A. (2019) Novel chitosan-Nafion composite for fabrication of highly sensitive impedimetric and colorimetric As(III) aptasensor. Biosensors and Bioelectronics, **131**(February), 1–8. [online] https://doi.org/10.1016/j.bios.2019.01.059.

Bülbül, G., Hayat, A., Mustafa, F., and Andreescu, S. (2018) DNA assay based on Nanoceria as Fluorescence Quenchers (NanoCeracQ DNA assay). Scientific Reports, **8**(1), 2426. [online] http://www.nature.com/articles/s41598-018-20659-9.

Chowdhury, U. K., Biswas, B. K., Chowdhury, T. R., Samanta, G., Mandal, B. K., Basu, G. C., Chanda, C. R., Lodh, D., Saha, K. C., Mukherjee, S. K., Roy, S., Kabir, S., Quamruzzaman, Q., and Chakraborti, D. (2000) Groundwater arsenic contamination in Bangladesh and West Bengal, India. Environmental Health Perspectives, **108**(5), 393–397.

Chung, C. J., Huang, Y. L., Huang, Y. K., Wu, M. M., Chen, S. Y., Hsueh, Y. M., and

433 Chen, C. J. (2013) Urinary arsenic profiles and the risks of cancer mortality: A
434 population-based 20-year follow-up study in arseniasis-endemic areas in Taiwan.
435 Environmental Research, **122**, 25–30. [online]
436 http://dx.doi.org/10.1016/j.envres.2012.11.007.
437 Clancy, T. M., Hayes, K. F., and Raskin, L. (2013) Arsenic waste management: A
438 critical review of testing and disposal of arsenic-bearing solid wastes generated
439 during arsenic removal from drinking water. Environmental Science and
440 Technology, **47**(19), 10799–10812.
441 Das, J. and Sarkar, P. (2016) A new dipstick colorimetric sensor for detection of
442 arsenate in drinking water. Environ. Sci.: Water Res. Technol., **2**(4), 693–704.
443 [online] http://xlink.rsc.org/?DOI=C5EW00276A.
444 Flora, S. J. S. (2015) *Handbook of Arsenic Toxicology*, © Academic Press 2015.
445 Hafuka, A., Nagasato, T., and Yamamura, H. (2019) Application of Graphene Oxide for
446 Adsorption Removal of Geosmin and 2-Methylisoborneol in the Presence of
447 Natural Organic Matter. International journal of environmental research and public
448 health, **16**(11), 1–8.
449 Kamei-Ishikawa, N., Segawa, N., Yamazaki, D., Ito, A., and Umita, T. (2017) Arsenic
450 removal from arsenic-contaminated water by biological arsenite oxidation and

chemical ferrous iron oxidation using a down-flow hanging sponge reactor. Water Science and Technology: Water Supply, **17**(5), 1249–1259.

Kaur, H., Kumar, R., Babu, J. N., and Mittal, S. (2015) Advances in arsenic biosensor development - A comprehensive review. Biosensors and Bioelectronics, **63**, 533–545. [online] http://dx.doi.org/10.1016/j.bios.2014.08.003.

Lakatos, M., Matys, S., Raff, J., and Pompe, W. (2015) Colorimetric As (V) detection based on S-layer functionalized gold nanoparticles. Talanta, **144**, 241–246. [online] http://dx.doi.org/10.1016/j.talanta.2015.05.082.

Liu, B. and Liu, J. (2015) Comprehensive Screen of Metal Oxide Nanoparticles for DNA Adsorption, Fluorescence Quenching, and Anion Discrimination. ACS Applied Materials and Interfaces, **7**(44), 24833–24838.

Liu, B. and Liu, J. (2014) DNA adsorption by magnetic iron oxide nanoparticles and its application for arsenate detection. Chemical Communications, **50**(62), 8568. [online] http://xlink.rsc.org/?DOI=C4CC03264K.

Lopez, A., Zhang, Y., and Liu, J. (2017) Tuning DNA adsorption affinity and density on metal oxide and phosphate for improved arsenate detection. Journal of Colloid and Interface Science, **493**, 249–256. [online] http://dx.doi.org/10.1016/j.jcis.2017.01.037.

Matsunaga, K., Okuyama, Y., Hirano, R., Okabe, S., Takahashi, M., and Satoh, H. (2019) Development of a simple analytical method to determine arsenite using a DNA aptamer and gold nanoparticles. Chemosphere, **224**, 538–543. [online] https://linkinghub.elsevier.com/retrieve/pii/S0045653519304060.

Muppidathi, M., Perumal, P., Ayyanu, R., and Subramanian, S. (2019) Immobilization of ssDNA on a metal-organic framework derived magnetic porous carbon (MPC) composite as a fluorescent sensing platform for the detection of arsenate ions. The Analyst, **144**(9), 3111–3118.

Pautler, R., Kelly, E. Y., Huang, P. J. J., Cao, J., Liu, B., and Liu, J. (2013) Attaching DNA to nanoceria: Regulating oxidase activity and fluorescence quenching. ACS Applied Materials and Interfaces, **5**(15), 6820–6825.

Pena-Pereira, F., Villar-Blanco, L., Lavilla, I., and Bendicho, C. (2018) Test for arsenic speciation in waters based on a paper-based analytical device with scanometric detection. Analytica Chimica Acta, **1011**, 1–10. [online] https://doi.org/10.1016/j.aca.2018.01.007.

Singh, R., Singh, S., Parihar, P., Singh, V. P., and Prasad, S. M. (2015) Arsenic contamination, consequences and remediation techniques: A review. Ecotoxicology and Environmental Safety, **112**, 247–270. [online]

http://dx.doi.org/10.1016/j.ecoenv.2014.10.009.

USEPA (2018) National Primary Drinking Water Regulations. [online] https://www.epa.gov/ground-water-and-drinking-water/national-primary-drinking-water-regulations.

Wang, L., Huang, Z., Liu, Y., Wu, J., and Liu, J. (2018) Fluorescent DNA Probing Nanoscale MnO2: Adsorption, Dissolution by Thiol, and Nanozyme Activity. Langmuir, **34**(9), 3094–3101.

WHO (2011) *Guidelines for Drinking-Water Quality - Fourth Edition*, [online] http://scholar.google.com/scholar?hl=en&btnG=Search&q=intitle:Health+Criteria+and+Other+Supporting+Information#1%5Cnhttp://scholar.google.com/scholar?hl=en&btnG=Search&q=intitle:Health+criteria+and+other+supporting+information%231.

Wu, Y., Liu, L., Zhan, S., Wang, F., and Zhou, P. (2012a) Ultrasensitive aptamer biosensor for arsenic(iii) detection in aqueous solution based on surfactant-induced aggregation of gold nanoparticles. Analyst, **137**(18), 4171–4178. [online] http://dx.doi.org/10.1039/C2AN35711A.

Wu, Y., Liu, L., Zhan, S., Wang, F., and Zhou, P. (2012b) Ultrasensitive aptamer biosensor for arsenic(iii) detection in aqueous solution based on surfactant-induced

505 aggregation of gold nanoparticles. The Analyst, **137**(18), 4171–4178. [online]
506 http://xlink.rsc.org/?DOI=c2an35711a.
507 Xu, X., Wang, L., Zou, X., Wu, S., Pan, J., Li, X., and Niu, X. (2019) Highly sensitive
508 colorimetric detection of arsenite based on reassembly-induced oxidase-mimicking
509 activity inhibition of dithiothreitol-capped Pd nanozyme. Sensors and Actuators B:
510 Chemical, **298**(July), 126876. [online] https://doi.org/10.1016/j.snb.2019.126876.
511 Zhan, S., Yu, C. M., and Lv, C. J. (2014) Colorimetric Detection of Trace Arsenic (III)
512 in Aqueous Solution Using Arsenic Aptamer and Gold Nanoparticles. Australian
513 Journal of Chemistry, **67**, 813–818.
514 Zong, C. and Liu, J. (2019) The Arsenic-Binding Aptamer Cannot Bind Arsenic:
515 Critical Evaluation of Aptamer Selection and Binding. Analytical Chemistry, **91**,
516 10887–10893.
517
518

519 Table S1: Concentration of ions (μM) in groundwater samples. “Bef” and “Aft” indicate
520 the samples before and after cation-exchange treatment, respectively. The ions
521 concentrations were measured by ICP-MS.

Ions	GW	
	Bef	Aft
B	-	-
Na	940	1,904
Mg	590	0.0667
Al	1.69	0.40
P	<0.00	<0.00
K	128	0.62
Ca	1,085	<0.00
Mn	0.242	<0.00
Fe	3.68	<0.00
Cu	0.09	<0.00
Zn	0.35	<0.00
As	<0.00	0.04

522

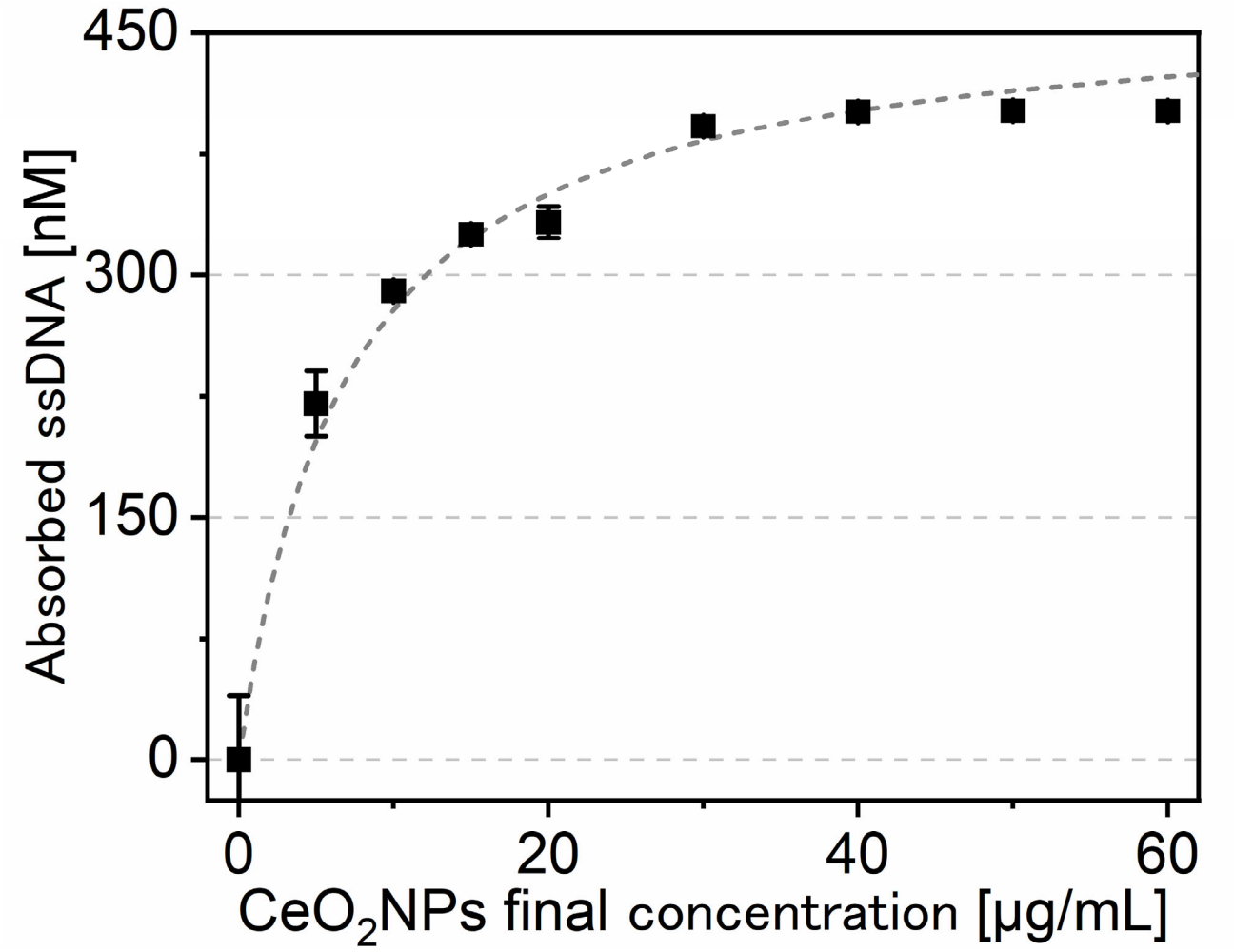

Figure S1: Adsorbed ssDNA as a function of the final CeO_2NP concentrations. The dotted line is the Langmuir isotherm.

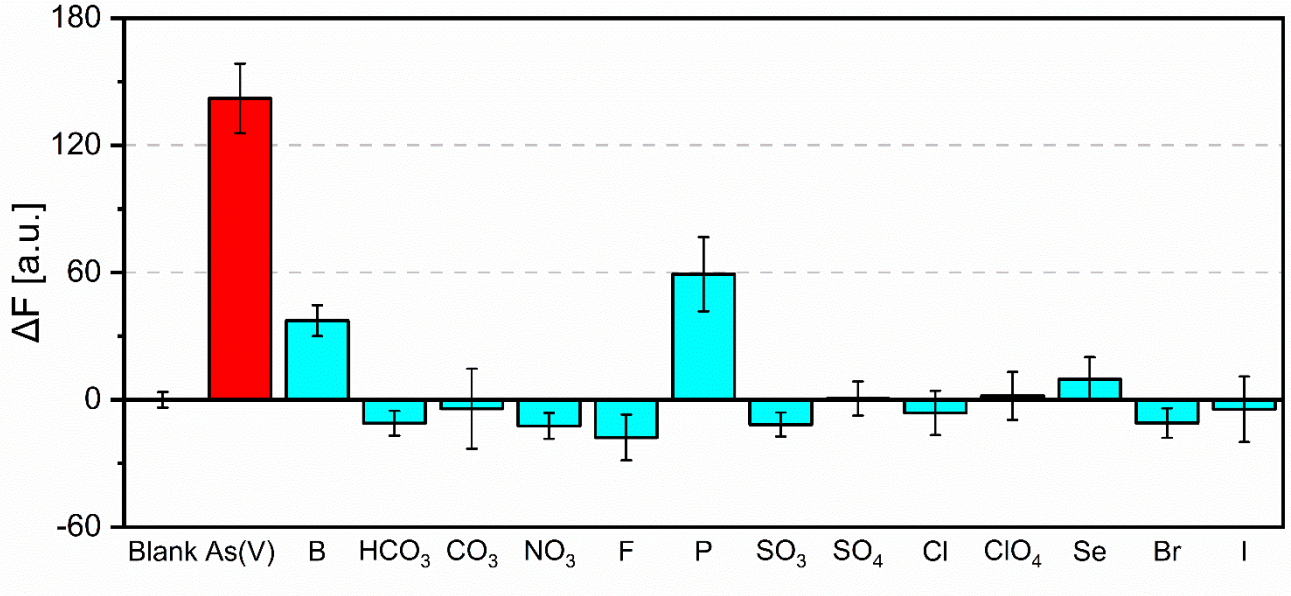

Figure S2: Method selectivity for anions. The concentration of As(V) was 10 µM and the others were 100 µM.

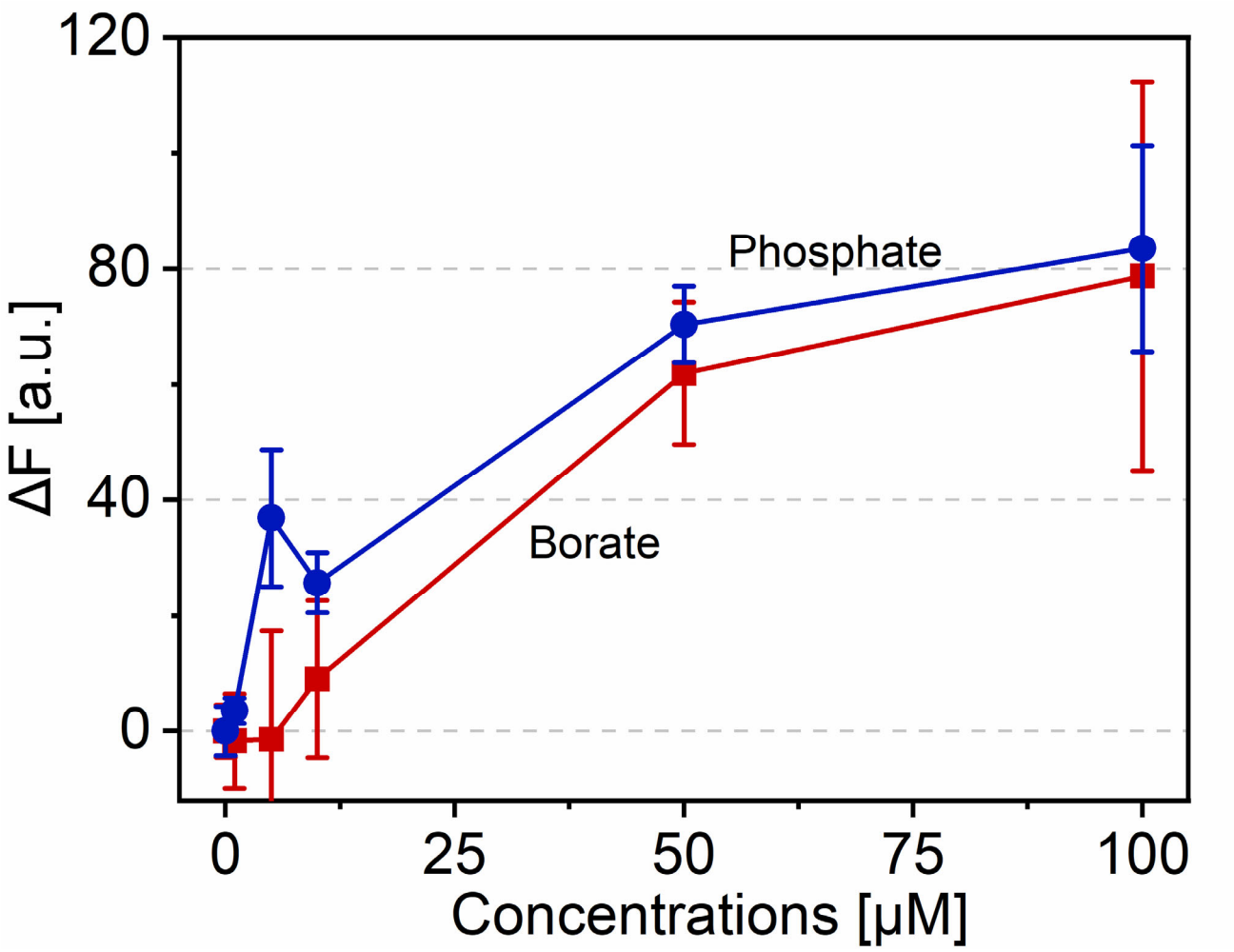

Figure S3: Effect of borate and phosphate on this method.

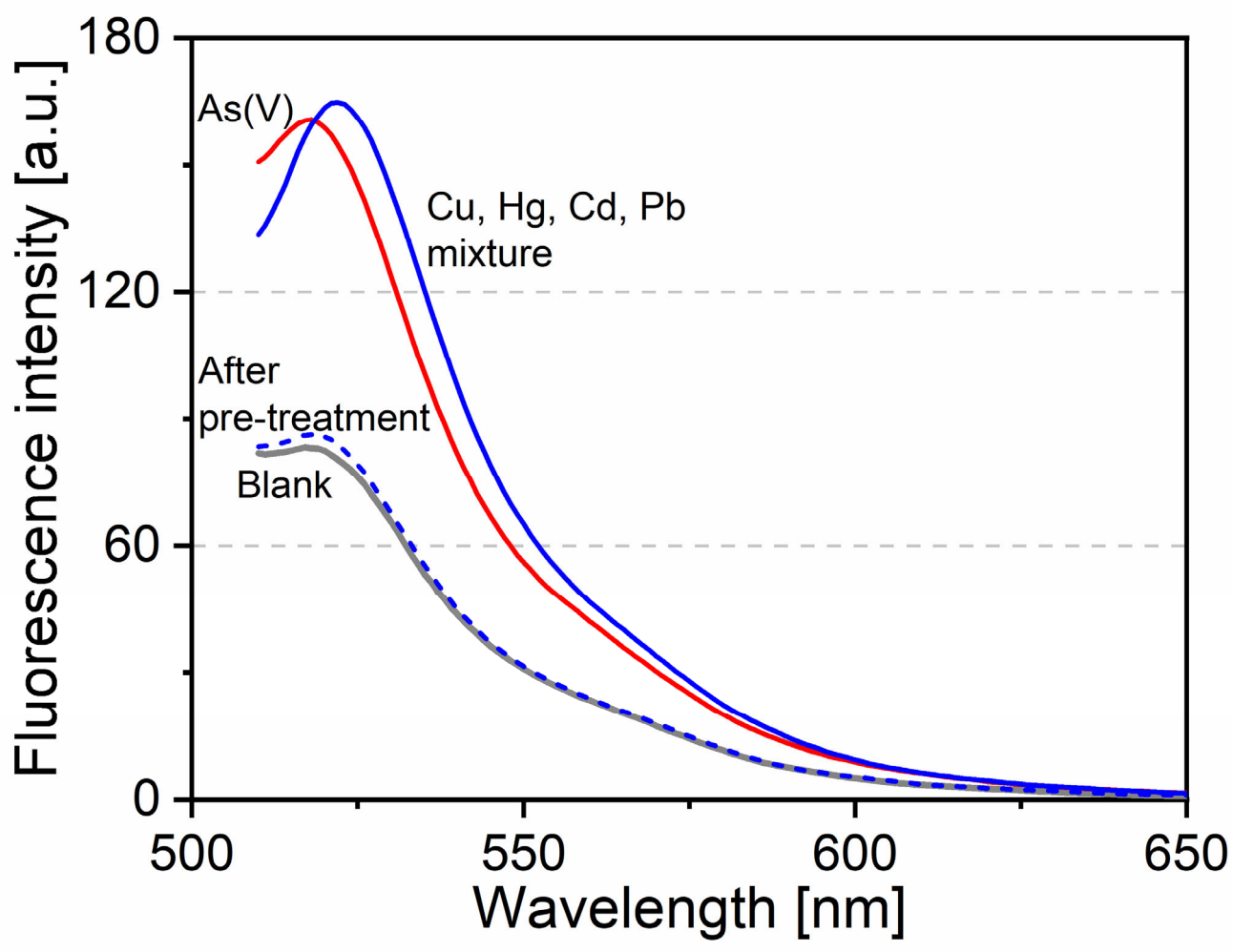

Figure S4: The effect of pre-treatment (cation-exchange) via inhibitor.

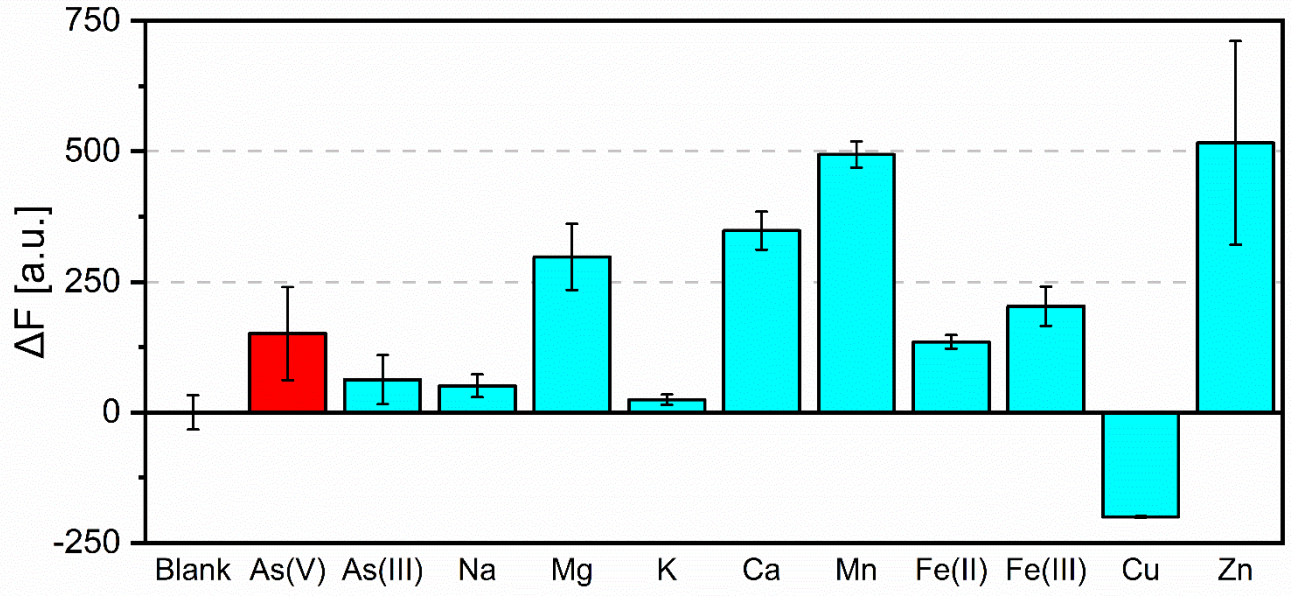

Figure S5: Effect of the metal ions that contain in groundwater at high concentration. The concentration of As(V) was 10 μM and the others were 100 μM.